Theory of Axial Compressor Blade Rows at Subsonic and Transonic Speeds," *AIAA Journal*, Vol. 8, No. 7, July 1970, pp. 1275–1283.

[3] Goldstein, S., "On the Vortex Theory of Screw Propellers," *Proceedings of the Royal Society of London*, Ser. A, Vol. 123, No. 792, April 6, 1929, pp. 440–465.

[4] Reissner, H., "On the Vortex Theory of the Screw Propeller," *Journal of the Aeronautical Sciences*, Vol. 5, No. 1, Nov. 1937, pp. 1–7.

[5] Okurounmu, O. and McCune, J. E., "Transonic Lifting Surface Theory for Axial Compressors," K213580-1, March 1971, United Aircraft Research Labs., East Hartford, Conn.

[6] Namba, M., "Small Disturbance Theory of Rotating Subsonic and Transonic Cascades," presented at the First International Symposium on Air Breathing Engines, Marseilles, France, June 19–23, 1972.

[7] McCune, J. E. and Okurounmu, O., "Three-Dimensional Flow in Transonic Axial Compressor Blade Rows," presented at the International Symposium on the Fluid Mechanics and Design of Turbomachinery, Pennsylvania State Univ., University Park, Pa., Aug. 1970.

[8] McCune, J. E., "Three-Dimensional Theory of Axial Compressor Blade Rows—Application to Subsonic and Supersonic Flows," *Journal of the Aerospace Sciences*, Vol. 25, No. 9, Sept. 1958, pp. 544–560.

[9] Weinig, F. S., "Theory of Two-Dimensional Flow through Cascades," *Princeton Series on High Speed Aerodynamics and Jet Propulsion*, Vol. 10, Princeton Univ. Press, Princeton, N.J., 1964, Sec. B, pp. 24–50.

[10] Horlock, J. H., "Axial Flow Compressors," *Fluid Mechanics and Thermodynamics*, Butterworths, London, 1958, pp. 48–51.

[11] McCune, J. E. and Dharwadkar, S. P., "Lifting Line Theory for Subsonic Axial Compressor Rotors," GTL 110, July 1972, Gas Turbine Lab., MIT, Cambridge, Mass.

OCTOBER 1974 AIAA JOURNAL VOL. 12, NO. 10

Part II—Transonic Compressor

The authors' three-dimensional, inviscid, linearized lifting surface theory of compressible flow past an axial compressor rotor is applied to transonic compressors. From the general solution, quasi-two-dimensional limiting forms are obtained for a supersonic blade section. The latter consists of an equivalent actuator-disk type flow due to the azimuthally averaged wake, plus the local two-dimensional supersonic cascade flow. The actual flow is shown to depart considerably from these quasi-two-dimensional flows, even for uniformly loaded rotors. These departures are due to two major factors: namely, the propagation of acoustic waves, and the occurrence of wake induced resonance. These waves influence the flow at all sections of the blade, thus eliminating the sharp differences that would otherwise exist between subsonic and supersonic blade sections. The resonant modes are treated by inclusion of certain nonlinear effects, and the acoustic pressure field is investigated and related to the rotor geometry and aerodynamics. Camber-line profiles are obtained for transonic rotors under specified loading distributions, and blade forms are shown to be very sensitive to the presence or absence of a wake, for a specified mean loading. For uniformly loaded transonic rotors, the blade camber becomes reversed near the sonic radius.

I. Introduction

In part I of the present theory,[1] the three-dimensional, inviscid, linearized lifting surface solution for compressible flow past an axial compressor blade row has been presented. It was shown that, by averaging the three-dimensional flow in the azimuthal direction, the resulting axisymmetric flow showed features of the well-known axisymmetric through-flow (actuator disk) theory. In particular, when the relative Mach number is everywhere subsonic, the general three-dimensional theory was reducible to a quasi-two-dimensional limiting form which was shown to consist of an actuator disk-type flow, on which was superposed the local two-dimensional cascade flow about the blade section. Departures of the actual flow from these quasi-two-dimensional limiting forms were shown to be primarily due to the presence of individual trailing vortices, that is, the rotor wake. Thus, for a uniformly loaded rotor, these quasi-two-dimensional approximations adequately represented the actual flow at each blade section.

These conclusions have recently been reinforced by Namba.[2] Although Namba's assumptions are the same as in the present work, his solution is based on a pressure dipole representation of the blade surfaces, from which the disturbance pressure and the perturbed field everywhere is then sought.

There has always been some doubt as to the applicability of the assumption of quasi-two-dimensionality to transonic rotors.[3] McCune[4] has studied the problem of transonic flow through a nonlifting axial compressor rotor for small values of the thickness to chord ratio. In the study, the blade thickness distribution was represented by radial source spikes of varying strength in the radial direction, and it was shown that the interference between various sections of the blades was considerable, the flow at each section being nowhere near to being quasi-two-dimensional. The primary reason for this radical departure from quasi-two-dimensionality was the acoustic resonance of certain eigenmodes which, when excited, drastically alter the flow at all sections of the blade row.

In the present paper, we make a similar investigation of the lifting transonic rotor, in which the blades, though having camber, will be assumed to have zero thickness. We stay, as before, within the framework of an inviscid, linearized theory. Within this framework, the complete problem is solved by superposition of the solutions of the thickness and lifting problems. For the lifting problem, we identify two major causes of large departures of the actual flow from quasi-two-dimensionality. The first is, as in the thickness problem, the excitation of propagating acoustic eigenmodes when the relative Mach number at the tip sections becomes supersonic. These modes, which propagate whether or not there is a wake behind the rotor make their presence felt at all radial sections, thus altering the essential pattern of the flow even at the hub sections where the relative Mach number is subsonic.

The second cause of departures from quasi-two-dimensionality is the wake. As in the subsonic case, the presence of trailing helical vortex sheets behind the rotor introduces additional induced velocities at each blade section. In the transonic case, however, the wake plays the additional role that it excites propagating acoustic modes, some of which, under certain conditions can become resonant, that is, have very large amplitudes within the linear theory; and when such resonance is excited, the interference between the different radial sections of the blade becomes greatly intensified. Since transonic operation always

involves resonance, or near resonance, of one or more of these modes, strong interference between different radial sections must be considered a basic feature of transonic rotors. A consequence of the above is that sharp differences in the character of the flow between the subsonic and supersonic sections of the blade row, which would be expected from quasi-two-dimensional considerations, do not really exist in a transonic rotor, as these tend to be smoothed out by the strong spanwise crossflow.

The propagating acoustic modes referred to above can be associated with the well-known "spinning modes" in cylindrical ducts which have been studied by several authors.[5-8] The usefulness of these studies is, however, limited by the fact that the pressure field is not directly predicted in terms of the rotor aerodynamics. Thus the pressure field must, in effect, be prescribed at a reference plane normal to the rotor axis, or in terms of effective "multipole" sources not readily interpretable in relation to the compressor's aerodynamic properties. In the present study, the pressure field derives naturally from the analysis of the three-dimensional flowfield around the compressor, so that the aerodynamic factors responsible for their generation are easily identified.

In what follows we shall, from the general three-dimensional solution, obtain the quasi-two-dimensional limiting form at supersonic blade sections, and compare this with the known form at the subsonic sections. The former will be interpreted in terms of an equivalent actuator-disk type flow, on which is superposed the local supersonic cascade flow about the blade section. The inadequacy of the previous forms for approximating the actual flows, even for wakeless rotors, will be demonstrated, and the three-dimensional solutions will be used to compute the camber-line profiles in transonic operation, for specified blade loading distributions. Finally, the pressure field will be examined in relation to the loading and the acoustic energy of the propagating modes estimated. An interesting feature of transonic operation will be discussed, which is the possibility of camber reversal at some section within the annulus, depending on the loading distribution.

The off-design problem, namely that of finding the loading distribution and the disturbance field for a prescribed blade geometry, has been treated by Namba.[2]

II. General Three-Dimensional Solution

The lifting surface velocity potential for the three-dimensional flow in the rotor passages, valid for both subsonic and transonic flows, is already given in Ref. 1 as

$$\Phi^u(\rho,z,\theta)=\frac{B}{2\pi\beta^2}\int_0^{C_{ax}}d\xi\left\{\sum_{k=1}^{\infty}-\frac{\gamma_{ok}(\xi)}{2\lambda_{ok}}e^{\lambda_{ok}(z-\omega\xi/U)}R_0(K_{ok}\eta)+\sum_{n=1}^{\infty}\sum_{k=1}^{\infty}\left[(-1)^n\frac{h_{nk}(\xi)}{\lambda_{nk}}+\frac{i\beta^2(-1)^n}{nB}[h_{nk}(\xi)+\gamma_{nk}(\xi)]\right]\times e^{inB(\theta-\omega\xi/U)}e^{(inBM^2/\beta^2+\lambda_{nk})(z-\omega\xi/U)}R_{nB}(K_{nk}\eta)\right\}\equiv\frac{B}{2\pi\beta^2}\int_0^{C_{ax}}d\xi[\delta\Phi^u];\qquad z\leqq 0 \tag{1}$$

$$\Phi^d(\rho,z,\theta)=\frac{B}{2\pi\beta^2}\int_0^{C_{ax}}d\xi\left\{\bar\gamma(\xi)\left(z-\frac{\omega\xi}{U}\right)+\frac{\beta^2\gamma(\eta,\xi)}{\cos\phi}\zeta_I-\sum_{k=1}^{\infty}\frac{\gamma_{ok}(\xi)}{2\lambda_{ok}}e^{-\lambda_{ok}(z-\omega\xi/U)}R_0(K_{ok}\eta)+\sum_{n=1}^{\infty}\sum_{k=1}^{\infty}\frac{2i\beta^2}{nB}(-1)^n h_{nk}(\xi)\,e^{inB\zeta}R_{nB}(K_{nk}\eta)+\sum_{n=1}^{\infty}\sum_{k=1}^{\infty}\left[(-1)^n\frac{h_{nk}(\xi)}{\lambda_{nk}}-\frac{i\beta^2(-1)^n}{nB}[h_{nk}(\xi)+\gamma_{nk}(\xi)]\right]\times e^{inB(\theta-\omega\xi/U)}e^{(inBM^2/\beta^2-\lambda_{nk})(z-\omega\xi/U)}R_{nB}(K_{nk}\eta)\right\}\equiv\frac{B}{2\pi\beta^2}\int_0^{C_{ax}}d\xi[\delta\Phi^d];\qquad z\geqq\omega c_{ax}/U \tag{2}$$

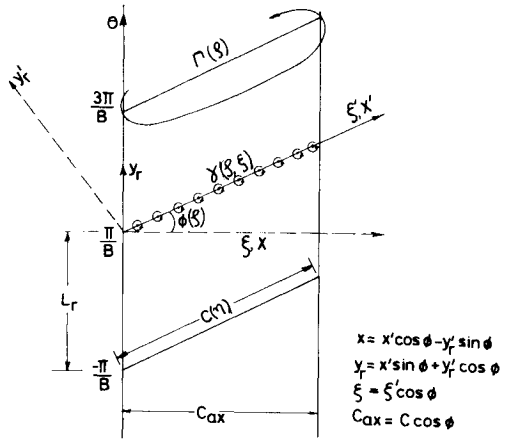

Fig. 1 Systems of coordinates and bound vortices.

$$\Phi^i(\rho,z,\theta)=\frac{B}{2\pi\beta^2}\left\{\int_0^x\delta\Phi^d\,d\xi+\int_x^{C_{ax}}\delta\Phi^u\,d\xi\right\};\qquad 0\leqq z\leqq\frac{\omega c_{ax}}{U} \tag{3}$$

The coordinate system in these and subsequent expressions is as shown in Fig. 1, which is a cascade view at a radial section of the annulus. (r, x, θ) is a right-handed coordinate system in the radial, axial, and azimuthal directions, respectively, with corresponding dimensionless forms $(\rho, z, \theta) \equiv (\omega r/U, \omega x/U, \theta)$, where ω, U are, respectively, the rotor angular velocity and the axial velocity of the airstream far upstream of the rotor. The Mach number corresponding to U is M and $\beta^2 \equiv 1-M^2$. The blade loading is represented by the bound vortex distribution $\gamma(\rho, \xi)$ along the local chord of the B blades of the rotor. The integrated loading $\Gamma(\rho)$ at any radius, and the average loading $\bar\gamma(\xi)$ at any chordwise position are given by

$$\Gamma(\rho)=\int_0^{C_{ax}}\gamma(\rho,\xi)\frac{d\xi}{\cos\phi} \tag{4}$$

and

$$\bar\gamma(\xi)=\frac{2}{1-h^2}\int_h^1\frac{\gamma(\eta,\xi)}{\cos\phi}\eta\,d\eta \tag{5}$$

where $\eta = r/r_T = \rho/\rho_T$; $h = \rho_H/\rho_T$, and the subscripts H, T denote hub and tip conditions, respectively.

The coefficients $\gamma_{ok}(\xi)$, $\gamma_{nk}(\xi)$; $h_{nk}(\xi)$, which will be henceforth written without their arguments, are, respectively, the coefficients of the Fourier-Bessel expansion of the loading distribution $\gamma(\eta, \xi)/\cos\phi$, and the wake functions $\chi_n(\eta, \xi)$ in a series of the orthonormal characteristic functions $R_0(K_{ok}\eta)$, $R_{nB}(K_{nk}\eta)$ which will also be henceforth written simply as R_0, R_{nB}. All these functions and coefficients are fully described in Refs. 9 and 10. The coordinate ζ appearing in Eq. (2) is defined by $\zeta \equiv \theta - z$, and is constant along the helix of advance of the blades, on which it takes the values $\pm\pi/B$, $\pm 3\pi/B$, $\pm 5\pi/B$, etc.

Finally, λ_{ok}, λ_{nk} are axial eigenvalues, given by

$$\lambda_{nk}=\frac{1}{\beta}\left(\frac{K_{nk}^2}{\rho_T^2}-\frac{n^2B^2M^2}{\beta^2}\right)^{1/2} \tag{6}$$

where the K_{nk}'s are the radial eigenvalues for which the radial velocity vanishes at the hub and shroud.

The velocity components (u, v, w) in the axial, azimuthal, and radial directions immediately follow from Eqs. (1-3) through the relations

$$u=\frac{\omega}{U}\frac{\partial\Phi}{\partial z},\qquad v=\frac{\omega}{\rho U}\frac{\partial\Phi}{\partial\theta}\qquad w=\frac{\omega}{U\rho_T}\frac{\partial\Phi}{\partial\eta} \tag{7}$$

As already discussed in Ref. 9, when the tip relative Mach number exceeds unity, imaginary values of λ_{nk} can occur (for $n > 0$), giving rise to acoustic modes which propagate upstream

and downstream. For $n > 0$, only a finite number of the λ_{nk}'s can be imaginary, the rest being real and thus giving rise to axially decaying modes. If we are however interested only in the azimuthal mean of the flow velocity components, then even these propagating modes average out to zero, so that in so far as defining an equivalent axisymmetric flow as a first approximation to the actual flow upstream and downstream of the rotor, there is no essential difference between the subsonic and transonic flow cases. Thus, the azimuthally averaged velocities upstream and downstream of the rotor are identical with those given in Ref. 1, for the completely subsonic flow. In particular, the induced velocity components at the blade row by the equivalent actuator disk are those given in Ref. 1, namely

$$u'_{ad}(0) = \Gamma \sin\phi/2L_r\beta^2 - \sin\phi(\Gamma - \bar{\Gamma})/2L_r\beta^2 \tag{8}$$

$$v'_{ad}(0) = \beta_r{}^2 \cos\phi\Gamma/2L_r\beta^2 + \sin^2\phi(\Gamma - \bar{\Gamma})/2L_r\beta^2\cos\phi \tag{9}$$

In either Eqs. (8) or (9), the first term represents the contribution of the local loading, while the second is the contribution of the azimuthally averaged wake (note that it is zero for wakeless rotors) and is associated with mean stream surface deflections of the flowfield.

III. Induced Velocities and Quasi-Two-Dimensional Limiting Forms

The velocity components u', v' within the blade row, in the x', y_r', coordinates, respectively, are easily obtained from Eqs. (1–3, and 7), and an easy coordinate transformation as illustrated in Fig. 1. Using the abbreviated notation

$$\psi(z, \theta; \xi) = \theta - \frac{\omega\xi}{U} + \frac{M^2}{\beta^2}\left(z - \frac{\omega\xi}{U}\right) \tag{10}$$

we obtain

$$u'(\eta, z, \theta) = \frac{B\omega}{4\pi\beta^2 U(1+\rho^2)^{1/2}}\left[\bar{\Gamma} + \left\{\int_0^x d\xi - \int_x^{C_{ax}} d\xi\right\}\bar{\gamma} + \sum_{k=1}^{\infty}\left\{\int_0^x d\xi\, e^{-\lambda_{ok}(z-\omega\xi/U)} - \int_x^{C_{ax}} d\xi\, e^{\lambda_{ok}(z-\omega\xi/U)}\right\}\gamma_{ok} R_0 + 2i\sum_{n=1}^{\infty}\sum_{k=1}^{\infty}(-1)^n \int_0^{C_{ax}} d\xi\, e^{inB\psi}\, e^{-\lambda_{nk}|z-\omega\xi/U|} \times \left\{\frac{\lambda_{nk}\beta^2}{nB}(\gamma_{nk}+h_{nk}) + \frac{nBh_{nk}}{\beta^2\lambda_{nk}}\right\} R_{nB} + 2\sum_{n=1}^{\infty}\sum_{k=1}^{\infty}(-1)^n \left\{\int_0^x d\xi\, e^{-\lambda_{nk}(z-\omega\xi/U)} - \int_x^{C_{ax}} d\xi\, e^{\lambda_{nk}(z-\omega\xi/U)}\right\} e^{inB\psi}\gamma_{nk} R_{nB}\right] \tag{11}$$

$$v'(\eta, z, \theta) = \frac{-B\omega\rho}{4\pi\beta^2 U(1+\rho^2)^{1/2}}\left[\bar{\Gamma} - \beta^2\left(1+\frac{1}{\rho^2}\right)\Gamma(\rho) + \left\{\int_0^x d\xi - \int_x^{C_{ax}} d\xi\right\}\left\{\bar{\gamma}(\xi) - \beta^2\left(1+\frac{1}{\rho^2}\right)\frac{\gamma(\eta,\xi)}{\cos\phi}\right\} + \sum_{k=1}^{\infty}\left\{\int_0^x d\xi\, e^{-\lambda_{ok}(z-\omega\xi/U)} - \int_x^{C_{ax}} d\xi\, e^{\lambda_{ok}(z-\omega\xi/U)}\right\}\gamma_{ok} R_0 + 2i\sum_{n=1}^{\infty}\sum_{k=1}^{\infty}(-1)^n \int_0^{C_{ax}} d\xi\, e^{inB\psi}\, e^{-\lambda_{nk}|z-\omega\xi/U|} \times \left\{\frac{\lambda_{nk}\beta^2}{nB}(\gamma_{nk}+h_{nk}) + \frac{nB}{\lambda_{nk}\beta^2}\left(M^2 - \frac{\beta^2}{\rho^2}\right)h_{nk}\right\} R_{nB} + 2\sum_{n=1}^{\infty}\sum_{k=1}^{\infty}(-1)^n \left\{\int_0^x d\xi\, e^{-\lambda_{nk}(z-\omega\xi/U)} - \int_x^{C_{ax}} d\xi\, e^{\lambda_{nk}(z-\omega\xi/U)}\right\} \times \left\{\left(M^2 - \frac{\beta^2}{\rho^2}\right)\gamma_{nk} - \beta^2\left(1+\frac{1}{\rho^2}\right)h_{nk}\right\} e^{inB\psi} R_{nB} + 4\beta^2\left(1+\frac{1}{\rho^2}\right)\sum_{n=1}^{\infty}(-1)^n e^{inB\zeta}\int_0^x \chi_n(\eta,\xi)\, d\xi\right] \tag{12}$$

Further, the radial velocity component w is easily shown to be

$$w(\eta, z, \theta) = \frac{B\omega}{2\pi\beta^2 U\rho_T}\left[\int_0^x d\xi\beta\frac{\partial}{\partial\eta}\left(\frac{\gamma}{\cos\phi}\right)\zeta_l - \sum_{k=1}^{\infty}\frac{\beta\rho_T}{2}\int_0^{C_{ax}} d\xi\, e^{-\lambda_{ok}|z-\omega\xi/U|}\gamma_{ok} R_0' + \sum_{n=1}^{\infty}\sum_{k=1}^{\infty}(-1)^n 2i\beta^2\int_0^x d\xi\frac{K_{nk}}{nB}h_{nk}\, e^{inB\zeta} R_{nB}' + \sum_{n=1}^{\infty}\sum_{k=1}^{\infty}(-1)^n\int_0^{C_{ax}} d\xi\frac{K_{nk}h_{nk}}{\lambda_{nk}} e^{-\lambda_{nk}|z-\omega\xi/U|}\, e^{inB\psi} R_{nB}' - \sum_{n=1}^{\infty}\sum_{k=1}^{\infty}(-1)^n i\beta^2\left\{\int_0^x d\xi\, e^{-\lambda_{nk}(z-\omega\xi/U)} - \int_x^{C_{ax}} d\xi\, e^{\lambda_{nk}(z-\omega\xi/U)}\right\}\frac{K_{nk}}{nB}(h_{nk}+\gamma_{nk})\, e^{inB\psi} R_{nB}'\right] \tag{13}$$

A. Resonance

The terms that could become unusually large as the rotor tip speed exceeds unity are those involving λ_{nk} in the denominator. The amplitudes of these terms are seen to be invariably proportional to h_{nk}/λ_{nk}, so that the resonance in transonic rotors is invariably wake induced. When any such term becomes resonant, the radial velocity component w can become quite large, adding to the three-dimensional effects produced by the propagating, nonresonant acoustic modes. Within the framework of the present linear theory, the vanishing of a particular λ_{nk} would imply an infinite amplitude for such modes as described previously. There is therefore the necessity to modify the theory, if a finite amplitude for these modes is to be obtained. The approach used by McCune[4] for the thickness problem was to include viscous effects near resonance, and thus obtain a modified value of λ_{nk}, dependent on the Reynolds number, reducing to Eq. (6) as $Re \to \infty$, while remaining finite at the resonant condition of Eq. (6) for finite Reynolds numbers.

In the present work, we modify the axial eigenvalues near resonance by inclusion of certain nonlinear terms in the equations of motion. If in the acoustic wave equation in duct fixed coordinates, we retain the second-order time-dependent terms, and then transform to rotor-fixed coordinates, we obtain

$$\beta^2\Phi_{zz} + \Phi_{\rho\rho} + (1/\rho)\Phi_\rho + (1/\rho^2)(1-M^2\rho^2)\Phi_{\theta\theta} - 2M^2\Phi_{\theta z} = \frac{2\omega}{a^2}\left[\Phi_\rho\Phi_{\rho z} + \Phi_\rho\Phi_{\rho\theta} + (1/\rho^2)\Phi_\theta\Phi_{\theta z} + (1/\rho^2)\Phi_\theta\Phi_{\theta\theta} + \Phi_z\Phi_{zz} + \Phi_z\Phi_{z\theta}\right] \tag{14}$$

where all the nonlinear terms are on the right-hand side, and a is the speed of sound. Next, we examine the two-dimensional limiting form of Eq. (14), by confining attention to a blade section at fixed radius, and imagining the section to be part of an infinite aspect ratio, two-dimensional cascade. In that limit, derivatives with respect to ρ vanish, and the resulting equation is most conveniently expressed in the coordinate system (x', y_r') as

$$\Phi_{x'x'}(1-M_r^2) + \Phi_{y_r'y_r'} = (2M_r^2/U_r)(\Phi_{x'}\Phi_{x'x'} + \Phi_{y_r'}\Phi_{x'y_r'}) \tag{15}$$

with $M_r = U_r/a$ being the local relative Mach number. Thus, near $M_r = 1$, a significant correction to the coefficient of $\Phi_{x'x'}$ on the left-hand side of Eq. (15) can be obtained by retaining the first term on the right, and dropping the second. Thus, we have

$$\Phi_{x'x'}(1-M_r^2) + \Phi_{y_r'y_r'} = (2M_r^2/U_r)\Phi_{x'}\Phi_{x'x'}; \qquad M_r \to 1 \tag{16}$$

We now assume that in the neighborhood of the blades, and near $M_r = 1$, the chordwise derivative of the chordwise velocity component, $\Phi_{x'x'}$ is constant. This assumption is analogous to that made by Oswatitsch[11] in determining the flow about a half body of revolution at the speed of sound. Maeder and Thommen[12] later showed that this assumption is actually quite good at all speeds for the calculation of flow about slender bodies. Thus, if we replace $\Phi_{x'x'}$ in the right-hand side of Eq. (15) by $\Phi_{x'x'} = K$, where K is understood to mean some appropriate

average of $\Phi_{x'x'}$ throughout the region around the blades, we have

$$\Phi_{x'x'}(1-M_r^2)+\Phi_{y_r'y_r'}=(2M_r^2/U_r)K\Phi_{x'} \tag{17}$$

Transforming Eq. (17) back to the (ρ, θ, z) coordinate system, and adding the linear terms involving radial derivatives, we obtain the appropriate modified differential equation, near resonance as

$$\beta^2\Phi_{zz}+\Phi_{\rho\rho}+(1/\rho)\Phi_\rho+(1/\rho^2)(1-M^2\rho^2)\Phi_{\theta\theta}-2M^2\Phi_{\theta z}=\Lambda(\Phi_z+\Phi_\theta) \tag{18}$$

where

$$\Lambda=2M^2K/\omega \tag{19}$$

If a solution is sought to Eq. (18), having the same form as the present solution, namely

$$\Phi_{nk}=R_{nB}(K_{nk}\eta)\,e^{(inBM^2/\beta^2\pm\lambda_{nk}{}^*)z}\,e^{inB\theta} \tag{20}$$

the resulting expression for $\lambda_{nk}{}^*$ is

$$\lambda_{nk}{}^*=\pm\left\{\frac{\Lambda}{2\beta^2}+\frac{1}{2}\left[\frac{\Lambda^2}{\beta^4}+4\left(\lambda_{nk}{}^2+\frac{inB\Lambda}{\beta^4}\right)\right]^{1/2}\right\} \tag{21}$$

which is the required modified λ_{nk} as the latter approaches zero. We note that

$$\lim_{\lambda_{nk}\to 0}\lambda_{nk}{}^*=\pm\left\{\frac{\Lambda}{2\beta^2}+\frac{1}{2\beta^2}(\Lambda^2+4inB\Lambda)^{1/2}\right\} \tag{22}$$

It remains to find an expression for Λ in terms of the rotor geometry and aerodynamic loading.

First, we note that

$$\Phi_{x'x'}=\left(\frac{\omega}{U}\right)^2\cos^2\phi(\Phi_{zz}+2\Phi_{z\theta}+\Phi_{\theta\theta}) \tag{23}$$

If we average this as required in the radial, azimuthal, and axial directions, we obtain

$$K\equiv\overline{\Phi}_{x'x'}=\left(\frac{\omega}{U}\right)^2\langle\cos^2\phi\rangle\overline{\Phi}_{zz} \tag{24}$$

where $\langle\cos^2\phi\rangle$ is the spanwise average of $\cos^2\phi$. Thus

$$\overline{\frac{\partial u}{\partial x}}\equiv\overline{\Phi_{xx}}=\frac{1}{\langle\cos^2\phi\rangle}\frac{\omega\Lambda}{2M^2} \tag{25}$$

Using Eq. (25), we may relate the averaged axial velocity change across the rotor to Λ, namely

$$\overline{\Delta u}=\bar{u}(c_{ax})-\bar{u}(0)=\frac{1}{\langle\cos^2\phi\rangle}\frac{\omega\Lambda}{2M^2}c_{ax} \tag{26}$$

Furthermore

$$\overline{r\Delta v}=B\bar{\Gamma}/2\pi \tag{27}$$

and using the fact that the perturbation density σ at any point is $\sigma=-(\sigma_{-\infty}/a^2)(Uu+\omega rv)$, we can write the averaged density change across the rotor as

$$\overline{\Delta\sigma}=-\frac{\sigma_{-\infty}}{a^2}(U\,\overline{\Delta u}+\omega r\overline{\Delta v})=-\frac{\sigma_{-\infty}}{a^2}\left\{\frac{\omega U\Lambda c_{ax}}{2M^2\langle\cos^2\phi\rangle}+\frac{\omega B\bar{\Gamma}}{2\pi}\right\} \tag{28}$$

Finally, using Eqs. (26) and (28), and imploring conservation of mass over the flow annulus between rotor leading and trailing edges, up to first order, we obtain

$$\Lambda=\frac{BUM^2\bar{\Gamma}}{\pi a^2\beta^2c_{ax}}\langle\cos^2\phi\rangle=\frac{(\phi_T-\phi_H)}{\rho_T(1-h)}\frac{BM^4}{\pi\beta^2}\frac{(\bar{\Gamma}/UL)}{(c_{ax}/L_T)} \tag{29}$$

where $\bar{\Gamma}$ as before, is the mean loading. Equations (21) and (29) complete the treatment of resonant modes. Two points are worthy of note. First, it is not necessary that λ_{nk} vanish exactly before applying the preceding modification. As soon as $|\lambda_{nk}{}^2|$ is less than a certain value, then the corresponding modes can be considered "resonant," and the preceding correction applied. In the present work, a mode is considered resonant when $|\lambda_{nk}{}^2|\leqq 0.002(nBM)^2/\beta^4$. Second, when the modification discussed above is used, the modified λ_{nk} is no longer either pure real or pure imaginary. It has both a real and imaginary part. This is important when we consider acoustic radiation, for it means that such modes are invariably eliminated from the far-field acoustic field, although they still play an active role in the near field, and particularly, in the velocity field within the rotor passages.

B. Quasi-Two-Dimensional Limit

Although the flow at any blade section in transonic flow is under no circumstances quasi-two-dimensional, it is nevertheless instructive to obtain these two-dimensional limiting forms, if only for the purpose of comparison with the actual flow. Of course, at subsonic sections of the blade, these limiting forms are those which have already been derived in Ref. 1.

At a supersonic section, in analogy to the procedure used in Ref. 1, we define a two-dimensional limiting form of the axial eigenvalue as $\lambda_r{}^n$ where

$$\lambda_r{}^n=\frac{nB}{\beta^2\rho}(1-M_r{}^2)^{1/2}\equiv\frac{inB}{\beta^2\rho}\mu_r \tag{30}$$

so that, since $M_r>1$, μ_r is real and positive. As before, we replace the λ_{nk}'s in Eqs. (11) and (12) by $\lambda_r{}^n$, neglect the wake terms, and use the notation

$y_r=r(\theta-\pi/B)$, $L_r=2\pi r/B$ (see Fig. 1), and

$$Y=y_r-\xi\tan\phi+\frac{M^2}{\beta^2}(x-\xi)\tan\phi=y_r+\frac{M^2x}{\beta^2}\tan\phi-\frac{\xi}{\beta^2}\tan\phi$$

The resulting expressions are

$$u'_{2D}(\eta,x,y_r)=\frac{\sin\phi}{2L_r\beta^2}\bar{\Gamma}+\frac{\sin\phi}{2L_r\beta^2}\left\{\int_0^x\frac{d\xi}{\cos\phi}\gamma(\eta,\xi)-\int_x^{C_{ax}}\frac{d\xi}{\cos\phi}\gamma(\eta,\xi)\right\}\left\{1+2\sum_{n=1}^{\infty}e^{2\pi n/L_r[-i(\mu_r/\beta^2)|x-\xi|+iY]}\right\}-\frac{\mu_r\cos\phi}{2L_r\beta^2}\int_0^{C_{ax}}\frac{d\xi}{\cos\phi}\gamma(\eta,\xi)\sum_{n=1}^{\infty}2\,e^{2\pi n/L_r[-i(\mu_r/\beta^2)|x-\xi|+iY]} \tag{31}$$

$$v'_{2D}(\eta,x,y_r)=-\frac{\sin^2\phi}{2L_r\beta^2\cos\phi}\bar{\Gamma}+\frac{\Gamma}{2L_r\cos\phi}-\frac{\mu_r{}^2\cos\phi}{2L_r\beta^2}\left\{\int_0^x\frac{d\xi}{\cos\phi}\gamma(\eta,\xi)-\int_x^{C_{ax}}\frac{d\xi}{\cos\phi}\gamma(\eta,\xi)\right\}\times\left\{1+2\sum_{n=1}^{\infty}e^{2\pi n/L_r[-i(\mu_r/\beta^2)|x-\xi|+iY]}\right\}+\frac{\mu_r\sin\phi}{2L_r\beta^2}\int_0^{C_{ax}}\frac{d\xi}{\cos\phi}\gamma(\eta,\xi)\cdot 2\sum_{n=1}^{\infty}e^{2\pi n/L_r[-i(\mu_r/\beta^2)|x-\xi|+iY]} \tag{32}$$

For comparison of Eqs. (31) and (32) with two-dimensional supersonic cascade theory, we recall the identity

$$1+2\sum_{n=1}^{\infty}\cos\frac{n\pi x}{l}\equiv 2l\sum_{m=-\infty}^{\infty}\delta(x-2ml)$$

where $\delta(x)$ is the Dirac delta function. If we transform to the (x', y_r') coordinates, note that

$$\beta^2\equiv\sin^2\phi-\mu_r{}^2\cos^2\phi \tag{33}$$

and use the relation

$$\delta(ax)=\frac{1}{|a|}\delta(x)$$

Equation (31) reduces to

$$u'_{2D}(\eta,x',y_r')=\frac{\bar{\Gamma}\sin\phi}{2L_r\beta^2}+\frac{\Gamma\mu_r\cos\phi}{2L_r(\sin^2\phi-\mu_r{}^2\cos^2\phi)}+\frac{1}{2}\int_0^{x'-y_r'\tan\phi}d\xi'\gamma(\eta,\xi')\sum_{m=-\infty}^{\infty}\times\delta[x'+\mu_r y_r'-mL_r(\sin\phi+\mu_r\cos\phi)-\xi']-\frac{1}{2}\int_{x'-y_r'\tan\phi}^{C}d\xi'\gamma(\eta,\xi')\sum_{m=-\infty}^{\infty}\times\delta[x'-\mu_r y_r'-mL_r(\sin\phi-\mu_r\cos\phi)-\xi'] \tag{34}$$

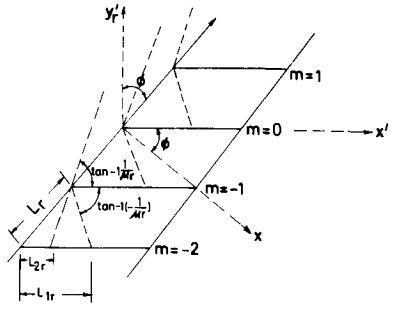

Fig. 2 Geometrical interpretation of L_{1r} and L_{2r} in supersonic flow.

We note that the discontinuities implied by the delta functions in Eq. (34) occur along the straight lines

$$\begin{aligned} x'+\mu_r y_r'-mL_r(\sin\phi+\mu_r\cos\phi)-\xi'=0 \\ x'-\mu_r y_r'-mL_r(\sin\phi-\mu_r\cos\phi)-\xi'=0 \end{aligned} \tag{35}$$

These lines are easily seen to be the right and left running families of Mach waves originating from the blade surface, and having slopes $-1/\mu_r$ and $+1/\mu_r$, respectively. These lines are marked I and II, respectively, in Fig. 2 which is a cascade development of the blade row in which $\phi(\rho)\equiv\tan^{-1}\rho$ is the local air angle.

If we define

$$L_{1r}\equiv L_r(\sin\phi+\mu_r\cos\phi), \qquad L_{2r}\equiv L_r(\sin\phi-\mu_r\cos\phi) \tag{36}$$

then L_{1r}, L_{2r} have the geometric interpretations shown in Fig. 2, and we may write Eq. (34) as

$$\begin{aligned} u'_{2D}(\eta,x',y_r') = {} & \frac{\Gamma\sin\phi}{2L_r\beta^2}-\frac{\sin\phi}{2L_r\beta^2}(\Gamma-\bar{\Gamma})+\frac{L_r\Gamma\mu_r\cos\phi}{2L_{1r}L_{2r}}+ \\ & \frac{1}{2}\int_0^{x'-y_r'\tan\phi} d\xi'\gamma(\eta,\xi')\sum_{m=-\infty}^{\infty}\delta(x'+\mu_r y_r'-mL_{1r}-\xi')- \\ & \frac{1}{2}\int_{z'-y_r'\tan\phi}^{C} d\xi'\gamma(\eta,\xi')\sum_{m=-\infty}^{\infty}\delta(x'-\mu_r y_r'-mL_{2r}-\xi') \end{aligned} \tag{37}$$

Similarly, it can be shown that Eq. (32) reduces to

$$\begin{aligned} v'_{2D}(\eta,x',y_r') = {} & -\frac{\mu_r^2\cos\phi\Gamma}{2L_r\beta^2}+\frac{\sin^2\phi(\Gamma-\bar{\Gamma})}{2L_r\beta^2\cos\phi}-\frac{L_r\Gamma\mu_r\sin\phi}{2L_{1r}L_{2r}}+ \\ & \frac{\mu_r}{2}\int_0^{x'-y_r'\tan\phi} d\xi'\gamma(\eta,\xi')\sum_{m=-\infty}^{\infty}\delta(x'+\mu_r y_r'-mL_{1r}-\xi')+ \\ & \frac{\mu_r}{2}\int_{x'-y_r'\tan\phi}^{C} d\xi'\gamma(\eta,\xi')\sum_{m=-\infty}^{\infty}\delta(x'-\mu_r y_r'-mL_{2r}-\xi') \end{aligned} \tag{38}$$

The above integrals are most conveniently expressed in terms of Heaviside's unit function $H(x)$, where $H(x)=0$, $x<0$, and $H(x)=1$, $x\geq 0$. Writing $\gamma(\eta,\xi')$ as $\gamma(\eta,\xi')[H(\xi')-H(\xi'-c)]$ and extending the limits in the integrals to infinity, we obtain, at the blade surface ($y_r'=0$)

$$\begin{aligned} u'_{2D}(\eta,x',y_r'=0+) = {} & \frac{\Gamma\sin\phi}{2L_r\beta^2}-\frac{\sin\phi}{2L_r\beta^2}(\Gamma-\bar{\Gamma})+\frac{L_r\Gamma\mu_r\cos\phi}{2L_{1r}L_{2r}}+ \\ & \frac{1}{2}\sum_{m=1}^{\infty}\gamma(\eta,x'-mL_{1r})[H(x'-mL_{1r})-H(x'-mL_{1r}-c)]- \\ & \frac{1}{2}\sum_{m=-\infty}^{0}\gamma(\eta,x'-mL_{2r})[H(x'-mL_{2r})-H(x'-mL_{2r}-c)] \end{aligned} \tag{39}$$

$$\begin{aligned} u'_{2D}(\eta,x',y_r'=0-) = {} & \frac{\Gamma\sin\phi}{2L_r\beta^2}-\frac{\sin\phi}{2L_r\beta^2}(\Gamma-\bar{\Gamma})+\frac{L_r\Gamma\mu_r\cos\phi}{2L_{1r}L_{2r}}+ \\ & \frac{1}{2}\sum_{m=0}^{\infty}\gamma(\eta,x'-mL_{1r})[H(x'-mL_{1r})-H(x'-mL_{1r}-c)]- \\ & \frac{1}{2}\sum_{m=-\infty}^{-1}\gamma(\eta,x'-mL_{2r})[H(x'-mL_{2r})-H(x'-mL_{2r}-c)] \end{aligned} \tag{40}$$

In the above, only the singularities which contribute to the respective integrals have been retained in the summation over m, the others being discarded.

The change in the u' velocity component across the blade surface is thus

$$\begin{aligned} \Delta u'_{2D}(\eta,x',y_r'=0) \equiv {} & u'_{2D}(\eta,x',y_r'=0+)- \\ & u'_{2D}(\eta,x',y_r'=0-)=\gamma(\eta,x')[H(x')-H(x'-c)] \end{aligned} \tag{41}$$

as would be expected. Also, only the $m=0$ term contributes to this jump in chordwise velocity component across the blade row. Similarly, it may be shown that, at the blade surface

$$\begin{aligned} v'_{2D}(\eta,x',y_r'=0\pm) = {} & -\frac{\mu_r^2\cos\phi\Gamma}{2L_r\beta^2}+\frac{\sin^2\phi(\Gamma-\bar{\Gamma})}{2L_r\beta^2\cos\phi}- \\ & \frac{L_r\Gamma\mu_r\sin\phi}{2L_{1r}L_{2r}}+\frac{\mu_r}{2}\gamma(\eta,x')[H(x')-H(x'-c)]+ \\ & \frac{\mu_r}{2}\sum_{m=1}^{\infty}\gamma(\eta,x'-mL_{1r})[H(x'-mL_{1r})-H(x'-mL_{1r}-c)]+ \\ & \frac{\mu_r}{2}\sum_{m=1}^{\infty}\gamma(\eta,x'+mL_{2r})\times \\ & [H(x'+mL_{2r})-H(x'+mL_{2r}-c)] \end{aligned} \tag{42}$$

so that the v' component is continuous across the blade row.

Equations (39) or (40) and Eq. (42) have the following interpretation. The first two terms of Eq. (39) are easily seen to be identical with Eq. (8), while the first two terms of Eq. (42) are easily shown to be identical with Eq. (9), since $\beta_r^2=-\mu_r^2$. These terms represent a modification of the basic flow by an equivalent axisymmetric flow replacing the actual flow. They are given by the same expressions, whether the flow is subsonic or transonic. The third terms in Eqs. (39) and (42) are peculiar to transonic flow. They represent an additional modification of the entering flow into the rotor due to the Mach waves originating from the leading edge of the blades and traveling upstream. The resultant of this latter perturbation is in the axial direction, and of magnitude $\Gamma\mu_r/2L_r\beta^2$, so that the net effect of all the upstream propagating Mach waves from the leading edges of all the blades is to change the entering air axial velocity by this magnitude. This is in agreement with two-dimensional supersonic cascade theory for blades of zero thickness and camber.[13] The remaining terms in these equations represent the local supersonic flow through the cascade.

In interpreting these terms, we refer to Fig. 3 where the summation index m now denotes each blade of the infinite two-dimensional cascade, and the straight blades shown represent the projections of the actual camber lines in the plane of the undisturbed relative flow. Let it be desired to find the upwash at a point such as P taken arbitrarily to be on the zeroth blade, since the flow pattern repeats from blade to blade. The upwash at P is influenced only through the disturbances from neighboring blades arriving along the Mach lines of either family passing through P, and also of course, by the disturbance originating at P itself. There is no contribution at P from reflected waves. The camber line of the blade continually adjusts to the influence of its neighbors in such a manner that incoming Mach waves are not reflected. This is a direct consequence of prescribing the chordwise loading in advance without regard to the inlet Mach number or rotational speed, and hence, the Mach wave locations. It is thus necessary for the camber line to continually adjust in order to remain consistent with the prescribed loading.

Now, looking at Eq. (42) and Fig. 3, the first 3 terms of the equation have already been discussed. The fourth term is the contribution of the local circulation at P itself to the upwash. The next term represents the sum of the interference by right running Mach waves, such as B_1P at P. For this particular geometry, only the $m=1$ term of the series is needed, the terms for higher m being zero by virtue of the Heaviside functions. Physically, this means that the next blade up is outside of the range of dependence of the point P, as shown in the figure. Looking at the $m=1$ term, we see that $(\mu_r/2)\gamma(\eta,x'-L_{1r})$ is the fluid turning at B_1 across the Mach wave B_1P due to the local circulation at B_1. Thus, by adding this turning to the fluid

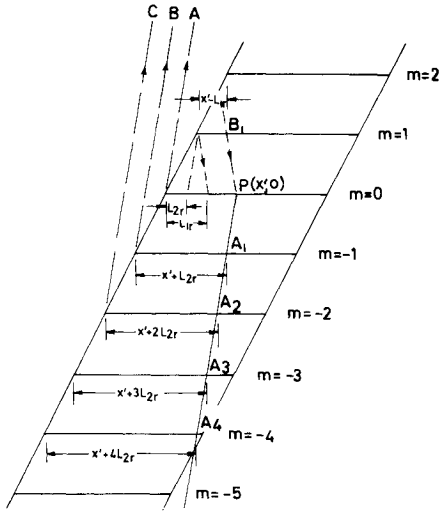

Fig. 3 Interference geometry between blades.

direction at P because of the local circulation there, we automatically cancel the wave that would have been reflected at P.

Similarly, the last term of Eq. (42) represents the sum of the interference produced at P by left running Mach waves $A_4A_3A_2A_1P$, the only contributing terms of the series being $m = 1, 2, 3,$ and 4. Again, $(\mu_r/2)\gamma(\eta, x'+4L_{2r})$ is the local fluid turning at A_4. Adding this to the local turning at A_3 eliminates the need for a reflected wave at A_3; and this sum represents the total turning at A_3 across the Mach wave A_3A_2. If we add this later sum to the local turning at A_2, we eliminate the need for a reflected wave at A_2 and so on. Thus, the net interference at P is obtained from the cumulative addition of the influence of such points as B_1, A_1, A_2, A_3, and A_4. A similar interpretation applies to Eqs. (39) and (40).

Equation (42) becomes degenerate at the sonic cylinder, where it vanishes identically for $\Gamma = \bar{\Gamma}$, that is, uniform loading. This is typical of two-dimensional linear theory. The full three-dimensional expressions are however not degenerate at the sonic radius. The advantage of deriving expressions such as Eqs. (39, 40, and 42) is to show the relationship of the present theory to two-dimensional theory. Since the actual flow departs considerably from two-dimensionality, these expressions are not useful for computational purposes, for which we must revert back to the full expressions, Eqs. (11) and (12). For details of the computational techniques, and discussions on the convergence of the series, the reader is referred to Ref. 10.

IV. Acoustic Pressure Field

The perturbation pressure at any point in the flowfield is readily shown to be

$$\hat{p} \equiv p - \langle p_{-\infty} \rangle = -\omega\sigma_{-\infty}(\partial\Phi/\partial z + \partial\Phi/\partial\theta) \tag{43}$$

where the symbol $\langle\ \rangle$ denotes a peripheral average. Thus, from Eqs. (1, 2, and 10), we obtain the pressure coefficients $C_p \equiv \hat{p}/(\sigma_{-\infty}U^2/2)$ upstream and downstream of the rotor as

$$C_p^{(u)}/C_{p_0} = \int_0^{C_{ax}} d\xi \left\{ \sum_{k=1}^{\infty} -\frac{\gamma_{ok}}{2\bar{\Gamma}} e^{\lambda_{ok}(z-\omega\xi/U)} R_0 + i\sum_{n=1}^{\infty}\sum_{k=1}^{\infty} (-1)^n \frac{h_{nk}}{\bar{\Gamma}}\left[\frac{nB}{\lambda_{nk}\beta^2} + \frac{\beta^2\lambda_{nk}}{nB}\right] e^{inB\psi}\, e^{\lambda_{nk}(z-\omega\xi/U)} R_{nB} + \sum_{n=1}^{\infty}\sum_{k=1}^{\infty} (-1)^n \frac{\gamma_{nk}}{\bar{\Gamma}}\left[\frac{i\beta^2\lambda_{nk}}{nB} - 1\right] \times e^{inB\psi}\, e^{\lambda_{nk}(z-\omega\xi/U)} R_{nB} \right\} \tag{44}$$

$$C_p^{(d)}/C_{p_0} = 1 + \int_0^{C_{ax}} d\xi \left\{ \sum_{k=1}^{\infty} \frac{\gamma_{ok}}{2\bar{\Gamma}} e^{-\lambda_{ok}(z-\omega\xi/U)} R_0 + i\sum_{n=1}^{\infty}\sum_{k=1}^{\infty} (-1)^n \frac{h_{nk}}{\bar{\Gamma}}\left[\frac{nB}{\lambda_{nk}\beta^2} + \frac{\beta^2\lambda_{nk}}{nB}\right] e^{inB\psi}\, e^{-\lambda_{nk}(z-\omega\xi/U)} R_{nB} + \sum_{n=1}^{\infty}\sum_{k=1}^{\infty} (-1)^n \frac{\gamma_{nk}}{\bar{\Gamma}}\left[\frac{i\beta^2\lambda_{nk}}{nB} - 1\right] \times e^{inB\psi}\, e^{-\lambda_{nk}(z-\omega\xi/U)} R_{nB} \right\} \tag{45}$$

where

$$C_{p_0} = (\langle p_{+\infty}\rangle - \langle p_{-\infty}\rangle)/(\sigma_{-\infty}U^2/2) = (-2\rho_T/\beta^2)\bar{\Gamma}/UL \tag{46}$$

If we take the peripheral averages of the above expressions, we obtain, for either subsonic or transonic flow

$$\left\langle \frac{C_p^{(u)}}{C_{p_0}} \right\rangle = \int_0^{C_{ax}} d\xi \left\{ \sum_{k=1}^{\infty} -\frac{\gamma_{ok}}{2\bar{\Gamma}} e^{\lambda_{ok}(z-\omega\xi/U)} R_0 \right\} \tag{47}$$

$$\left\langle \frac{C_p^{(d)}}{C_{p_0}} \right\rangle = 1 + \int_0^{C_{ax}} d\xi \left\{ \sum_{k=1}^{\infty} \frac{\gamma_{ok}}{2\bar{\Gamma}} e^{-\lambda_{ok}(z-\omega\xi/U)} R_0 \right\} \tag{48}$$

Far upstream and downstream of the rotor, the above-mentioned expressions decay to zero and one, respectively. This type of exponential decay is characteristic of axisymmetric through flow theory. The higher the axial Mach number, the larger the rate of decay.

Considering the three-dimensional far-field pressures, we note that for $M_T < 1$, $C_p^{(u)}/C_{p_0} \to 0$ while $C_p^{(d)}/C_{p_0} \to 1$ *as* $z \to \pm\infty$, respectively.

On the other hand, for $M_T > 1$, those modes for which λ_{nk} is imaginary propagate upstream and downstream. While propagating or "spinning" modes are associated with both the wake (through h_{nk}) and the bound vorticity (through γ_{nk}), we see that resonance can be excited only in the former, this happening when λ_{nk} (or μ_{nk}) becomes very small. Such cases are to be treated by the methods of Sec. III.A. As we have noted before, for each n, only the first several values of λ_{nk} can be imaginary. We therefore define k_n^* to be the maximum value of k, at each n, for which λ_{nk} is imaginary. Thus, for $k > k_n^*$, λ_{nk} is real and represents a decaying mode. Further, we adopt the convention that when λ_{nk} is imaginary, then $\lambda_{nk} \equiv i\mu_{nk}$. Finally, we assume that the loading $\gamma(\eta, \xi)/\cos\phi$ is expressible as $\Gamma(\eta)g(\xi)$, so that the coefficients $h_{nk}(\xi)$, $\gamma_{nk}(\xi)$ are related to the lifting line coefficients[8] H_{nk} and Γ_{nk} through

$$h_{nk}(\xi) = g(\xi)H_{nk}; \qquad \gamma_{nk}(\xi) = g(\xi)\Gamma_{nk} \tag{49}$$

Then, the far-field pressures in transonic flow can be written as

$$\frac{C_p^{(u)}}{C_{p_0}}(z \to -\infty) = \sum_{n=1}^{\infty}\sum_{k=1}^{k_n^*} \left\{ \frac{H_{nk}}{\bar{\Gamma}}\left(\frac{nB}{\beta^2\mu_{nk}} - \frac{\beta^2\mu_{nk}}{nB}\right) - \frac{\Gamma_{nk}}{\bar{\Gamma}}\left(\frac{\beta^2\mu_{nk}}{nB} + 1\right) \right\} R_{nB}\, e^{inB[\theta + \pi/B + \omega x/U(M^2/\beta^2 + \mu_{nk}/nB)]} \times \int_0^{C_{ax}} g(\xi)\, e^{-i(nB/\beta^2 + \mu_{nk})\omega\xi/U}\, d\xi \tag{50}$$

$$\frac{C_p^{(d)}}{C_{p_0}}(z \to +\infty) = 1 + \sum_{n=1}^{\infty}\sum_{k=1}^{k_n^*} \left\{ \frac{H_{nk}}{\bar{\Gamma}}\left(\frac{nB}{\beta^2\mu_{nk}} - \frac{\beta^2\mu_{nk}}{nB}\right) + \frac{\Gamma_{nk}}{\bar{\Gamma}}\left(1 - \frac{\beta^2\mu_{nk}}{nB}\right) \right\} R_{nB}\, e^{inB[\theta + \pi/B + \omega x/U(M^2/\beta^2 - \mu_{nk}/nB)]} \times \int_0^{C_{ax}} g(\xi)\, e^{-i(nB/\beta^2 - \mu_{nk})\omega\xi/U}\, d\xi \tag{51}$$

Now, let

$$\left\{ \frac{H_{nk}}{\bar{\Gamma}}\left(\frac{nB}{\beta^2\mu_{nk}} - \frac{\beta^2\mu_{nk}}{nB}\right) - \frac{\Gamma_{nk}}{\bar{\Gamma}}\left(\frac{\beta^2\mu_{nk}}{nB} + 1\right) \right\} R_{nB} \times \int_0^{C_{ax}} g(\xi)\, e^{-i(nB/\beta^2 + \mu_{nk})\omega\xi/U}\, d\xi \equiv A_{nk}^{(u)}(\eta)\, e^{i\alpha_{nk}^{(u)}} \tag{52}$$

and

$$\left\{\frac{H_{nk}}{\Gamma}\left(\frac{nB}{\beta^2\mu_{nk}}-\frac{\beta^2\mu_{nk}}{nB}\right)+\frac{\Gamma_{nk}}{\Gamma}\left(1-\frac{\beta^2\mu_{nk}}{nB}\right)\right\}R_{nB}\times \int_0^{C_{ax}} g(\xi)\,e^{-i(nB/\beta^2-\mu_{nk})\omega\xi/U}\,d\xi \equiv A_{nk}^{(d)}(\eta)\,e^{iz_{nk}^{(d)}} \quad (53)$$

then, Eqs. (50) and (51) can be written as (real parts implied)

$$\frac{C_p^{(u)}}{C_{p0}}(z\to-\infty)=\sum_{n=1}^{\infty}\sum_{k=1}^{k_n^*}A_{nk}^{(u)}(\eta)\,e^{i[nB\theta+P_{nk}^{(u)}(z)]} \quad (54)$$

$$\frac{C_p^{(d)}}{C_{p0}}(z\to+\infty)=1+\sum_{n=1}^{\infty}\sum_{k=1}^{k_n^*}A_{nk}^{(d)}(\eta)\,e^{i[nB\theta+P_{nk}^{(d)}(z)]} \quad (55)$$

where

$$P_{nk}^{(u)}(z)=\alpha_{nk}^{(u)}+n\pi+\left(\frac{nBM^2}{\beta^2}+\mu_{nk}\right)z$$

and (56)

$$P_{nk}^{(d)}(z)=\alpha_{nk}^{(d)}+n\pi+\left(\frac{nBM^2}{\beta^2}-\mu_{nk}\right)z$$

In Eqs. (54) and (55), the A_{nk}'s represent the amplitudes of the propagating modes, upstream or downstream, while the P_{nk}'s represent their phases. The rms of the amplitudes of these propagating pressure modes is of interest. To find these, we define

$$C_{pF}^{(u)}/C_{p0}\equiv C_p^{(u)}/C_{p0} \quad \text{and} \quad C_{pF}^{(d)}/C_{p0}\equiv C_p^{(d)}/C_{p0}-1 \quad (57)$$

where C_{pF} represents the fluctuating component of the far-field pressure coefficient, either upstream or downstream. It is easily shown that if C_{pF}/C_{p0} is averaged in the azimuthal direction, and also in the axial direction over a suitable length L_{ax} centered about some point x_o sufficiently far downstream or far upstream of the rotor, the result is

$$\left\langle\left\langle\left(\frac{C_{pF}}{C_{p0}}\right)^2\right\rangle\right\rangle_{(d)}^{(u)}(\eta)=\frac{1}{L_{ax}}\int_{x_o^{(u)}(d)-L_{ax}/2}^{x_o^{(u)}(d)+L_{ax}/2}\left\langle\left(\frac{C_{pF}}{C_{p0}}\right)^2\right\rangle_{(d)}^{(u)}dx=$$

$$\frac{1}{2}\sum_{n=1}^{\infty}\sum_{k=1}^{k_n^*}[A_{nk}^{(u)}{}_{(d)}]^2(\eta)+\mathscr{R}(x_0^{(u)}{}_{(d)},L_{ax},\eta) \quad (58)$$

where $\mathscr{R}(x_o^{(u)}{}_{(d)},L_{ax},\eta)$ is a small remainder term which tends to zero due to phase mixing, provided

$$|x_o^{(u)}{}_{(d)}|\gg L_{ax}\gg c_{ax}$$

V. Numerical Results

The geometry of the blade row, as well as the loading distributions remain as specified in Refs. 1 and 10. Briefly, $B=40$, $h=0.8$, $M=0.5$, $c_{ax}/L_T=1.06$, $g(\xi)=(8/\pi c_{ax})[\xi^*(1-\xi^*)]^{1/2}$ where $\xi^*=\xi/c_{ax}$ and

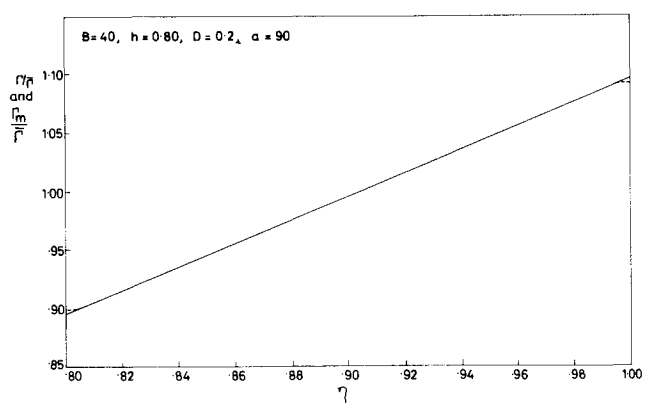

Fig. 4 Comparison of modified linear loading, Eq. (60) with purely linear loading, Eq. (59).

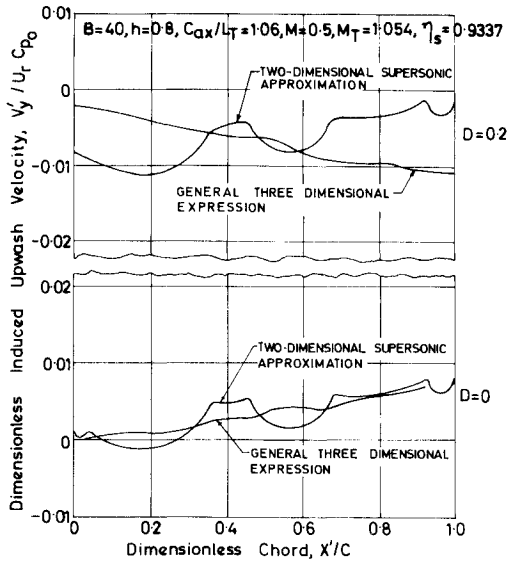

Fig. 5 Three-dimensional effects on the upwash velocity in transonic rotors for uniform loading ($D=0$) and nonuniform loading ($D=0.20$).

$$\Gamma(\eta)/\bar{\Gamma}=1-\frac{2D(1+h+h^2)}{3(1-h^2)}+\frac{D}{1-h}\eta \quad (59)$$

The parameter D is defined by $D=(\Gamma_T-\Gamma_H)/\bar{\Gamma}$, that is the fractional deviation from uniform loading.

As in Ref. 1, because

$$\sum_{n=1}^{\infty}\chi_n(nB\rho)$$

is singular at $\rho=\rho_H$ and $\rho=\rho_T$ when $d\Gamma/d\rho$ does not vanish at these points, it is necessary to modify the linear loading of Eq. (59) in such cases to meet these conditions. As before, the modified loading Γ_m, when $D\neq 0$, is given by

$$\Gamma_m(\eta)/\bar{\Gamma}=1-\frac{2D(1+h+h^2)}{3(1-h^2)}+\frac{D}{1-h}\eta+\frac{D}{1-h}\left\{\frac{\cosh[aB(1-\eta)]-\cosh[aB(\eta-h)]}{aB\sinh[aB(1-h)]}\right\} \quad (60)$$

and this is compared with the purely linear loading in Fig. 4, for $B=40$, $h=0.8$, $D=0.2$, and $a=9.0$. All quantities will be normalized with respect to C_{p0}, which can be specified arbitrarily, consistent with the linearizing assumptions of the theory. Further, the upwash will be normalized with $U_r=(U^2+\omega^2r^2)^{1/2}$, the local undisturbed relative velocity, while the camber-line profiles will be normalized with the local chord, $c(\eta)$. Figure 5 shows two sets of curves illustrating three-dimensional effects on the upwash velocity in transonic rotors, one set being for a uniformly loaded rotor ($D=0$), the other for a nonuniformly loaded rotor ($D=0.20$). In both sets, the quasi-two-dimensional approximation at the blade tip ($M_T=1.054$) as given by Eq. (42) with $\eta=1$, is compared with the general three-dimensional solution, Eq. (12). It is to be understood that these quasi-two-dimensional approximations include the induced velocities by the equivalent axisymmetric actuator disk flow, plus the local supersonic inviscid cascade flow. In particular, they include the effect of the azimuthally averaged wake, through the term involving $(\Gamma-\bar{\Gamma})$ in Eq. (42). In the case of uniform loading, the discrepancies in the two results are localized, but quite significant. The quasi-two-dimensional result overemphasizes the effect of individual Mach waves, which tend to be "smoothed" out by three-dimensional effects. This phenomenon may be described as "transonic three-dimensional relief." In the nonuniform loading case, the above effect is reinforced by the influence of the individual helical vortex sheets, so that the discrepancies are no longer merely local. The influence of these sheets is to increase the upwash near the leading edge and reduce it near the trailing

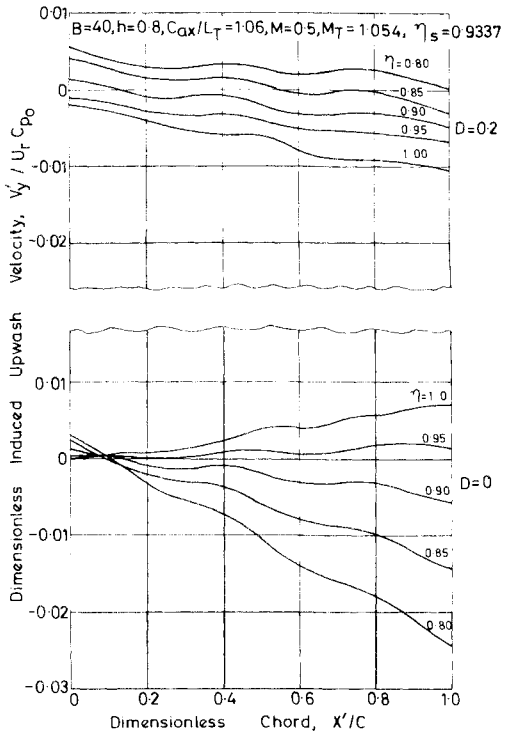

Fig. 6 Upwash velocity distributions for uniform loading ($D = 0$) and nonuniform loading ($D = 0.20$).

edge, relative to the local quasi-two-dimensional approximation. In what follows, we shall consider only the full three-dimensional results.

The effect of the transonic three-dimensional relief referred to previously is to eliminate the sharp qualitative differences in the nature of the flow at subsonic and supersonic sections, as would be expected from quasi-two-dimensional considerations only. Figure 6 shows the upwash velocities at various radial stations for both a uniformly loaded rotor, and a nonuniformly loaded one, for which $D = 0.20$. The tip Mach number is 1.054, and the sonic radius is at $\eta = \eta_s = 0.9337$. The influence of the wake is evident. In the uniformly loaded case, the upwash becomes quite

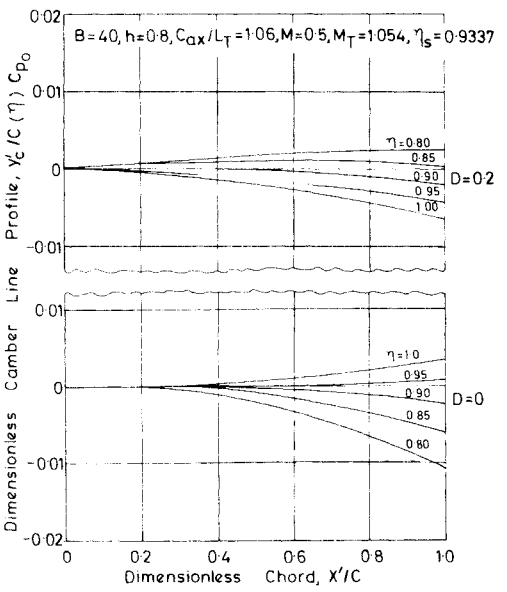

Fig. 7 Camber-line profiles for uniformly and nonuniformly loaded ($D = 0.2$) transonic rotors.

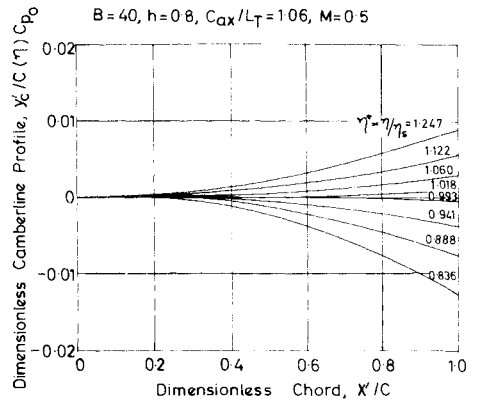

Fig. 8 Generalized camber-line profiles for transonic uniformly loaded rotors.

small near the sonic radius. The corresponding camber-line profiles for these two cases are shown in Fig. 7. For the wakeless rotor ($D = 0$) the camber becomes reversed at about the sonic radius, being positive for $\eta \lesssim \eta_s$ and negative for $\eta \gtrsim \eta_s$. For nonuniform loading, the camber may or may not become reversed at some section, depending on the details of the loading. The vastly different blade geometries required in these two cases is further evidence of the importance of the wake.

Another interesting feature of the uniformly loaded rotor is that, for a specified axial Mach number, rotor geometry, and chordwise loading, the camber-line profiles are relatively insensitive to the blade tip relative Mach number, and can be plotted with the single parameter $\eta^* = \eta/\eta_s$. Such a plot is shown in Fig. 8, in which individual curves are for different values of M_T.

Interest in the pressure field is in relation to the far-field noise, or acoustic radiation, where the far field is here taken to mean any region at a sufficiently far axial distance from the rotor that all the nonpropagating modes have decayed to negligible levels. Thus the amplitude of the pressure fluctuations become independent of distance in the far field, although this is not true of the phase. In the present work, far-field pressures have been computed at five chord length projections upstream of the blade leading edge, or downstream of the blade trailing edge. Figures 9 and 10 are typical of the upstream and downstream far-field pressure patterns, and are for $M_T = 1.054$. In these figures,

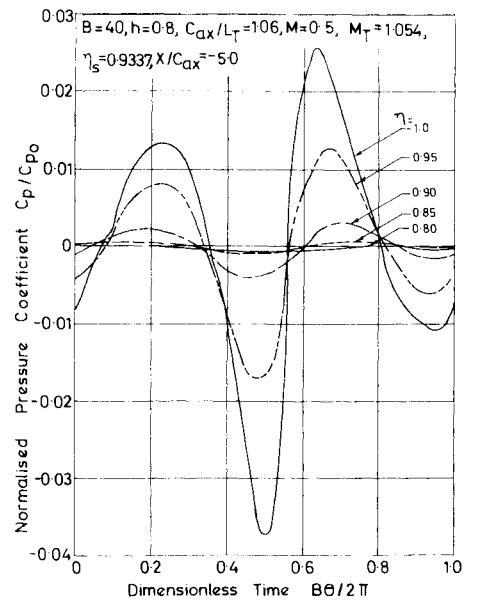

Fig. 9 Far-field acoustic radiation pattern upstream of rotor.

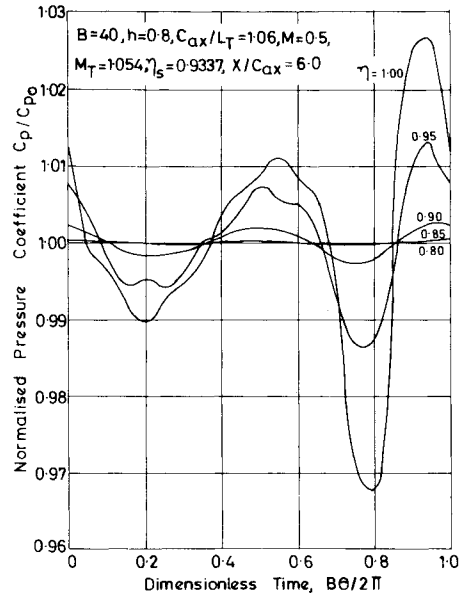

Fig. 10 Far-field acoustic radiation pattern downstream of rotor.

$B\theta/2\pi$ is the peripheral period between consecutive blades. These then are the so-called spinning modes and correspond to Eqs. (50) and (51). Near the root, the signal consists almost entirely of the (2,1) and (3,1) modes, the (2,1) mode being by far the more dominant. The signal at the tip contains many more harmonics, the most important of which are the (2,1) and (3,1) modes, but also including the (4,1), (5,1), (6,1), and (7,1), etc., modes. These pressure patterns are not very sensitive to the values of D (at least for the geometry under consideration). This is largely because the resonant or near resonant modes [in this case, the (1,1) mode] have been suppressed by the modifications described earlier, so that they do not contribute to the computed far-field noise, while the nonresonant but wake-induced propagating modes have amplitudes much smaller than those induced by the bound vortices, because $h_{nk} \ll \gamma_{nk}$. Moreover, the wake potential

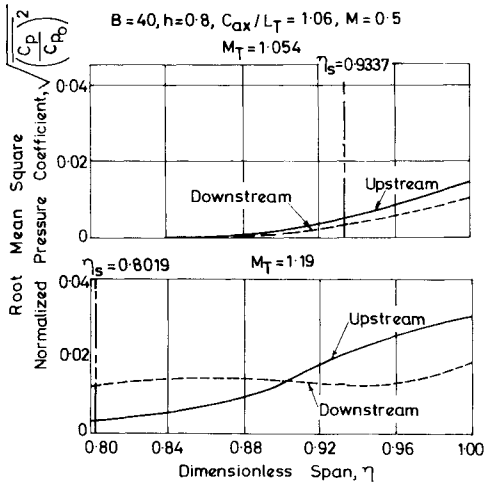

Fig. 11 Radial distribution of intensity of far-field acoustic radiation.

itself, since it depends on θ and z only through the combination $\zeta = \theta - z$, does not contribute to the first-order pressure. It does appear that additional nonlinear effects would have to be included in the analysis, in order to properly describe the far-field pressures, and bring out the influence of the wake.

As the tip relative Mach number increases, the number of radial modes (k index) that propagate for each n also increases thus raising the level of the far-field pressures at all radii. A measure of the intensity of the radiated noise can be obtained by computing the mean square value of the amplitudes of all the harmonics in the far-field pressure fluctuations, as defined by Eq. (57). The remainder term $\mathscr{R}(L_{ax}, \eta, x_o)$ is assumed negligible, since we are concerned only with the far field. These are shown in Fig. 11 for two different tip Mach numbers. At the lower tip Mach number, ($M_T = 1.054$), the sonic radius is at $\eta = 0.9337$, while at the larger tip Mach number ($M_T = 1.19$), the sonic radius is at $\eta = 0.8019$, very close to the hub. It is apparent that acoustic radiation is not confined to the supersonic section of the annulus although at low supersonic tip relative Mach numbers, it is small at radii much less than the sonic radius. The sound intensity builds up rapidly towards the rotor tip, and the radiation upstream and downstream appear to be generally of the same order of magnitude.

References

[1] Okurounmu, O. and McCune, J. E., "The Lifting Surface Theory of Axial Compressor Blade Rows: Part I—Subsonic Compressor," *AIAA Journal*, Vol. 12, No. 10, Oct. 1974, pp. 1363–1372.

[2] Namba, M., "Small Disturbance Theory of Rotating Subsonic and Transonic Cascades," 1st International Symposium on Air Breathing Engines, Marseilles, June 19–23, 1972.

[3] Marble, F. E., "Three Dimensional Flow in Turbo-Machines," *Princeton Series on High Speed Aerodynamics and Jet Propulsion*, edited by W. R. Hawthorne, Vol. 10, Sec. C, Princeton University Press, Princeton, N.J., 1964, pp. 83–116.

[4] McCune, J. E., "The Transonic Flow Field of an Axial Compressor Blade Row," *Journal of the Aerospace Sciences*, Vol. 25, Oct. 1958, pp. 616–626.

[5] Tyler, J. M. and Sofrin, T.-G., "Axial Flow Compressor Noise Studies," *SAE Transactions*, Vol. 70, 1962, pp. 209–232.

[6] Morfey, C. L., "Rotating Pressure Patterns in Ducts; Their Generation and Transmission," *Journal of Sound and Vibration*, Vol. 1, 1964, pp. 60–87.

[7] Slutsky, S., "Discrete Noise Generation and Propagation by a Fan Engine," AFOSR-UTIAS Symposium on Aerodynamic Noise, Univ. of Toronto, Toronto, Ontario, Canada, May 1968.

[8] Sofrin, T. G. and Pickett, G. F., "Multiple Pure Tone Noise Generated by Fans at Supersonic Tip Speeds," International Symposium on the Fluid Mechanics and Design of Turbomachinery, Pennsylvania State University, University Park, Pa., Aug. 1970.

[9] Okurounmu, O. and McCune, J. E., "Three-Dimensional Vortex Theory of Axial Compressor Blade Rows at Subsonic and Transonic Speeds," *AIAA Journal*, Vol. 8, No. 7, July 1970, pp. 1275–1283.

[10] Okurounmu, O. and McCune, J. E., "Transonic Lifting Surface Theory for Axial Flow Compressors," K213580-1, March 1971, United Aircraft Research Labs., East Hartford, Conn.

[11] Oswatitsch, K., "Flow Around Bodies of Revolution at Mach Number One," *Proceedings of the Conference on High Speed Aeronautics*, Polytechnic Institute of Brooklyn, Brooklyn, N.Y., Jan. 20–22, 1955, pp. 113–131.

[12] Maeder, P. F. and Thommen, H. U., "Linearized Transonic Flow about Slender Bodies of Revolution at Zero Incidences," TR W725, July 1957, Division of Engineering, Brown University, Providence, R.I.

[13] Ferri, A., "Aerodynamic Properties of Supersonic Compressors," *Princeton Series on High Speed Aerodynamics and Jet Propulsion*, edited by W. R. Hawthorne, Vol. 10, Sec. G, Princeton University Press, Princeton, N.J., 1964, pp. 381–431.